SCIENCE CHINA
Information Sciences

January 2019, Vol. 62 010202:1–010202:14
https://doi.org/10.1007/s11432-018-9581-y

• RESEARCH PAPER •
Special Focus on Guidance, Navigation and Control

UIF-based cooperative tracking method for multi-agent systems with sensor faults

Yingrong YU, Siting PENG, Xiwang DONG*, Qingdong LI & Zhang REN

Science and Technology on Aircraft Control Laboratory, School of Automation Science and Electrical Engineering, Beihang University, Beijing 100191, *China*

Received 27 June 2018/Accepted 19 July 2018/Published online 19 December 2018

Abstract For maneuvering target tracking with sensor faults, consensus-based distributed state estimation problems are studied herein. The communication status of the nonlinear system composed of multiple agents is described using the graph theory. Considering the impacts caused by sensor failures on measurement equations, a weighted average consensus-based unscented information filter (UIF) algorithm is proposed to improve tracking accuracy. Moreover, the estimation error for the investigated nonlinear system has been analyzed based on the stochastic boundedness theory to evaluate the proposed algorithm's performance and feasibility. Finally, simulation results are presented to assert the validity of the method.

Keywords unscented information filter, consensus theory, cooperative tracking, multi-agent system, stochastic boundedness

Citation Yu Y R, Peng S T, Dong X W, et al. UIF-based cooperative tracking method for multi-agent systems with sensor faults. Sci China Inf Sci, 2019, 62(1): 010202, https://doi.org/10.1007/s11432-018-9581-y

1 Introduction

Currently, maneuvering target tracking has been widely studied in both the military and civil fields for ballistic missile defense, intercept guidance, maritime surveillance, obstacle avoidance, bionic breakthroughs, among others [1–4]. Mobile vehicles including unmanned aerial vehicles (UAVs), missiles, robots, among others, can perform the tasks mentioned above (see example [5–8]). The research results in previous studies [9–12] indicate that a group of vehicles operating collaboratively exhibits many advantages such as precision, robustness, energy saving, and scalability, compared with an independent one.

Cooperative tracking aims at collecting and fusing the observations provided by mobile sensor networks, and designing estimation approaches to help a group of vehicles track the intended target. This tracking technology can improve the performance of the information fusion system, reduce the system response time, optimize resource allocation, save cost, and reduce the workload of operators. In the study of cooperative tracking, the group of mobile vehicles are always treated as a multi-agent system, such that most algorithms are not required to be specific to particular platforms [13]. An agent may represent a vehicle, a fixed sensor, a monitoring station, or a combination of them. The treatment can extend the universality and applicability of cooperative tracking algorithms.

Generally, the performance of the cooperative tracking technique for multi-agent systems is evaluated based on two criteria: (1) tracking accuracy; (2) node energy consumption. In recent years, international and domestic researchers have proposed new algorithms and schemes to improve the accuracy and reduce

* Corresponding author (email: xwdong@buaa.edu.cn)

the consumption simultaneously using different methods. The fault-tolerant cooperative tracking technique that is used for solving problems caused by environmental disturbance, sensor faults, poor accuracy of a single agent, or packet losses during communication, is a popular research topic [14, 15].

Hitherto, many significant results have been achieved by scholars. Focusing on the problem of observation packet loss, Li et al. [16] proposed a distributed state estimation method combining an optimal consensus-based filter and a suboptimal filter. Regarding intermittent observations, Tan et al. [17] adopted the cubature information filter for multiple sensor fusing to reduce the estimation errors. The distributed cubature information filter (CKF)-based algorithm for nonlinear estimation proposed in [18] proved its superiority compared with sigma point information filtering, and extended the application fields. By considering bounded noises, Chen et al. [19] adopted a unified mathematical model to describe the resource constraints and quantization effect, and designed a novel local estimator for time-varying systems.

Motivated by the achievements above, we herein propose an unscented information filter (UIF)-based cooperative tracking method for mobile sensor networks. The algorithm can be applied to solve the target's state estimation problems for nonlinear multi-agent systems with consideration of sensor failures. Moreover, the filter performance is evaluated according to the boundedness analysis of the estimation error. In this study, the sensors are assumed to fail intermittently during the course of tracking; hence, the systems cannot guarantee the stability and reliability of the measurements. If a sensor has malfunctioned completely and does not provide any output, the problem can be regarded as one for a new multi-agent system, whose agents are less than in the original system.

In contrast to the previous work on target tracking, the novelty of this study can be summarized as follows. (i) Unlike traditional consensus filtering methods, the proposed filtering approach combines the theory of weighted average consensus with UIF, and can be applied in nonlinear systems with sensor faults. In [16, 20–22], the systems were required to be linear or time invariant. Our simulation analyses proved that the filter adopted in this work is better than the other filters in [23–26]. The influence caused by sensor faults was not considered in [16–24]. (ii) The estimation error is analyzed and guaranteed to be bounded based on the stochastic stability lemma, which is challenging because of the information exchange among the group. The discussions about stochastic stability in [17, 18, 24–26] did not include the unscented information filter for systems with sensor failures.

The remainder of this article is organized as follows. The cooperative tracking problem for mobile sensor networks is formulated in Section 2. Section 3 provides the proposed cooperative tracking algorithm combining UIF and the weighted average consensus theory, and the analysis of the stochastic boundedness of the estimation error. Mathematical simulations in Section 4 indicate the performance of the proposed method. Conclusion is drawn in the end.

The following notations will be adopted throughout the article. Let $\mathbb{R}$ denote the real number field, and $\mathbb{R}^{n\times m}$ be the set of $n\times m$ real matrices. $\boldsymbol{I}_N$ represents an identity matrix of dimension N, and $\mathbf{1}_N$ represents a column vector all of whose elements are 1. $\|\cdot\|$ represents the Euclidean norm in $\mathbb{R}^n$. $\boldsymbol{P}^{\mathrm{T}}$ denotes the transpose of the matrix $\boldsymbol{P}$, and $\boldsymbol{P}^{-1}$ means inverse.

2 Problem formulation and representation

In this section, a detailed analysis of the cooperative tracking problem for mobile sensor networks with sensor failures is performed, and the maneuvering target model is constructed according to the assumed trajectory. Meanwhile, the graph theory is introduced to describe and study this multiple sensor networks.

2.1 Problem statement

For a typical target tracking system, the discrete-time nonlinear dynamic and measurement equations are as follows:

$$\begin{cases} \boldsymbol{x}_k = f(\boldsymbol{x}_{k-1}) + \boldsymbol{w}_{k-1}, \\ \boldsymbol{z}_k = h(\boldsymbol{x}_k) + \boldsymbol{v}_k. \end{cases} \tag{1}$$

Consider a nonlinear multi-agent system composed of N independent mobile vehicles tracking a single target (shown as a mass point), in which each vehicle is equipped with one sensor and the sensor failure may occur at odd intervals.

Therefore, the cooperative tracking problem considering the case of sensor failures can be described as follows:

$$\begin{cases} \boldsymbol{x}_k = f(\boldsymbol{x}_{k-1}) + \boldsymbol{w}_{k-1}, \\ \boldsymbol{z}_k^i = \lambda_k^i h^i(\boldsymbol{x}_k) + \boldsymbol{v}_k^i, \quad i = 1, 2, \ldots, N, \end{cases} \tag{2}$$

where $\boldsymbol{x}_k \in \mathbb{R}^n$ represents the state vector, $\boldsymbol{z}_k^i \in \mathbb{R}^m$ represents the observation vector associated with the i-th agent, and both $f(\cdot)$ and $h(\cdot)$ are continuously differentiable functions that represent the state transition and measurement, respectively. The covariance matrices of the process noise $\boldsymbol{w}_k$ and observation noise $\boldsymbol{v}_k^i$ are given by

$$\begin{cases} \boldsymbol{Q}_k = E\left[\boldsymbol{w}_k (\boldsymbol{w}_k)^{\mathrm{T}}\right], \\ \boldsymbol{R}_k^i = E\left[\boldsymbol{v}_k^i (\boldsymbol{v}_k^i)^{\mathrm{T}}\right], \end{cases} \tag{3}$$

where both $\boldsymbol{w}_k$ and $\boldsymbol{v}_k^i$ are white Gaussian sequences with zero mean; $\boldsymbol{Q}_k$ and $\boldsymbol{R}_k^i$ are the covariance matrices of $\boldsymbol{w}_k$ and $\boldsymbol{v}_k^i$, respectively.

We introduce the random variable λ_k^i into the measurement equation to describe the influence of sensor fault on target tracking. Equation $\lambda_k^i = 1$ means that the sensing device of the i-th agent performs well at time k; meanwhile, $\lambda_k^i = 0$ means that the malfunctioning of the sensor causes the observer failure (without useful output). The random variable λ_k^i obeys the following distribution rules:

$$\begin{cases} P(\lambda_k^i = 1) = 1 - \delta, \\ P(\lambda_k^i = 0) = \delta, \end{cases} \quad 0 \leqslant \delta \leqslant 1. \tag{4}$$

If $\{\lambda_k^i = 1, i = 1, 2, \ldots, N\}$ during the entire movement, the problem discussed herein can be simplified to the typical cooperative tracking based on the consensus theory. In addition, all the agents are assumed to be equipped with communication devices to share the observation information (state variables of the target) within the group.

2.2 Maneuvering target model

Without loss of generality, the typical maneuvering target models are discussed in a two-dimensional case. The coordinated turn (CT) model is typically used to describe the dynamic model of the maneuvering target

$$\begin{cases} \ddot{\xi} = -\omega \dot{\eta}, \\ \ddot{\eta} = \omega \dot{\xi}, \end{cases} \tag{5}$$

where ω represents the angular velocity; ξ and η denote the coordinate components in the X and Y directions of the rectangular coordinate system, respectively.

The state variable is described as $\boldsymbol{x} = [\xi, \dot{\xi}, \eta, \dot{\eta}]^{\mathrm{T}}$, and the state equation is

$$\dot{\boldsymbol{x}}(t) = \begin{bmatrix} \dot{\xi} \\ -\omega\dot{\eta} \\ \dot{\eta} \\ \omega\dot{\xi} \end{bmatrix} + \boldsymbol{B}\boldsymbol{w}(t) = \boldsymbol{A}\boldsymbol{x}(t) + \boldsymbol{B}\boldsymbol{w}(t), \tag{6}$$

where $\boldsymbol{w}(t)$ refers to the process noise,

$$\boldsymbol{A} = \begin{bmatrix} 0 & 1 & 0 & 0 \\ 0 & 0 & 0 & -\omega \\ 0 & 0 & 0 & 1 \\ 0 & -\omega & 0 & 0 \end{bmatrix}, \quad \boldsymbol{B} = \begin{bmatrix} 0 & 0 \\ 1 & 0 \\ 0 & 0 \\ 0 & 1 \end{bmatrix}.$$

The discrete-time model of the system's state equation has the following form:

$$\boldsymbol{X}_k = \begin{bmatrix} \xi_k \\ \dot{\xi}_k \\ \eta_k \\ \dot{\eta}_k \end{bmatrix} = \boldsymbol{F}\boldsymbol{X}_{k-1} + \boldsymbol{G}\boldsymbol{W}_{k-1}, \tag{7}$$

where

$$\boldsymbol{F} = \begin{bmatrix} 1 & \dfrac{\sin\omega T}{\omega} & 0 & -\dfrac{1-\cos\omega T}{\omega} \\ 0 & \cos\omega T & 0 & -\sin\omega T \\ 0 & \dfrac{1-\cos\omega T}{\omega} & 1 & \dfrac{\sin\omega T}{\omega} \\ 0 & \sin\omega T & 0 & \cos\omega T \end{bmatrix}, \quad \boldsymbol{G} = \begin{bmatrix} \dfrac{1-\cos\omega T}{\omega^2} & \dfrac{\sin\omega T-\omega T}{\omega^2} \\ \dfrac{\sin\omega T}{\omega} & \dfrac{\cos\omega T-1}{\omega} \\ \dfrac{\omega T-\sin\omega T}{\omega^2} & \dfrac{1-\cos\omega T}{\omega^2} \\ \dfrac{1-\cos\omega T}{\omega} & \dfrac{\sin\omega T}{\omega} \end{bmatrix},$$

$\boldsymbol{X}_k$ is the state of the target at the discrete time t_k, and T represents the sampling period.

Because $\omega T \approx 0$, one can obtain

$$\boldsymbol{G} \approx \begin{bmatrix} T^2/2 & 0 \\ T & 0 \\ 0 & T^2/2 \\ 0 & T \end{bmatrix}.$$

2.3 Communication

Communication is the basis of collaboration for multi-agent systems. In practice, the communication performance is limited by the capability of the available device, and deeply affected by the platform's motion and the complex battlefield environment.

Consider a multi-agent system composed of N independent mobile vehicles, and suppose that each agent can only exchange information effectively with its neighbors that are moving in its communication range. Each agent can be shown as a node. Therefore, the set of all the neighboring nodes of the i-th node can be expressed as $\boldsymbol{V}^i$. Further, a weighted undirected graph $\boldsymbol{G}[k] = \{\boldsymbol{V}, \boldsymbol{E}[k]\}$ is adopted to describe the communication relationships between the agents of the cooperative system. $\boldsymbol{V} = \{1, 2, \ldots, N\}$ represents the set of all the nodes, and edge $\boldsymbol{E} \subseteq \{(v_i, v_j) : v_i, v_j \in \boldsymbol{V}, i \neq j\}$ denotes the set of communication connections between i and j. The edge of graph $\boldsymbol{G}[k]$ is defined as $e_{ij} = (v_i, v_j)$. An edge e_{ij} is undirected if and only if $e_{ij}, e_{ji} \in \boldsymbol{E}[k]$, and information exchanges between them are completely equivalent.

We define the incidence matrix $\boldsymbol{A}[k]$ as follows:

$$\boldsymbol{A}_{ij}[k] = \begin{cases} 1, & \text{if } i \neq j \ \& \ (i,j) \subseteq \boldsymbol{E}[k], \\ 0, & \text{otherwise.} \end{cases} \tag{8}$$

Based on (8), let $\boldsymbol{L}[k] \in \mathbb{R}^{N\times N}$ be the Laplacian matrix of the graph $\boldsymbol{G}[k]$:

$$\boldsymbol{L}_{ij}[k] = \begin{cases} -\boldsymbol{A}_{ij}[k], & \text{if } i \neq j, \\ \displaystyle\sum_{j=1, j\neq i}^{N} \boldsymbol{A}_{ij}[k], & \text{if } i = j. \end{cases} \tag{9}$$

From the analyses of (8) and (9), when graph $\boldsymbol{G}[k]$ is undirected, $\boldsymbol{A}[k]$ and $\boldsymbol{L}[k]$ are symmetric matrices. To obtain the precise estimation of the target's state, it is necessary for each node to exchange information with its neighbors using distributed estimation methods. It is assumed that the graph $\boldsymbol{G}[k]$ discussed herein is not fully connected.

The following two problems for the discussed systems (2) are primarily studied in the remainder of the paper: (i) the method to design a cooperative tracking algorithm to improve the estimation performance considering the influence of λ_k^i; (ii) the method to prove the boundedness of the estimation error in mean square.

3 Primary results

For mobile sensor networks, cooperative tracking implies the collaboration among the nodes for the filter estimation regarding the target's state variables. An effective filtering algorithm must be designed to fuse the observations from different nodes and to obtain the optimal estimation.

3.1 Unscented information filter

We define an augmented state vector $\hat{\boldsymbol{x}}_{k|k}^{\mathrm{a}} = [\hat{\boldsymbol{x}}_k, \hat{\boldsymbol{w}}_k]^{\mathrm{T}}$. Similarly, the augmented covariance matrix is

$$\boldsymbol{P}_{k|k}^{\mathrm{a}} = \begin{bmatrix} \boldsymbol{P}_k & 0 \\ 0 & \boldsymbol{Q}_k \end{bmatrix}.$$

We select $2n+1$ sigma points as follows ($i = 1, \ldots, n$):

$$\begin{aligned} \boldsymbol{\chi}_{0,k}^{\mathrm{a}} &= \hat{\boldsymbol{x}}_{k|k}^{\mathrm{a}}, \\ \boldsymbol{\chi}_{i,k}^{\mathrm{a}} &= \hat{\boldsymbol{x}}_{k|k}^{\mathrm{a}} + \left[\sqrt{(n+\theta)\boldsymbol{P}_{k|k}^{\mathrm{a}}}\right]_i, \\ \boldsymbol{\chi}_{i+n,k}^{\mathrm{a}} &= \hat{\boldsymbol{x}}_{k|k}^{\mathrm{a}} - \left[\sqrt{(n+\theta)\boldsymbol{P}_{k|k}^{\mathrm{a}}}\right]_i. \end{aligned} \tag{10}$$

The corresponding weights for the mean and covariance are given by

$$\begin{aligned} W_0^{\mathrm{m}} &= \theta/(n+\theta), \\ W_i^{\mathrm{m}} &= 1/[2(n+\theta)], \\ W_0^{\mathrm{c}} &= \theta/(n+\theta) + (1-\alpha^2+\beta), \\ W_i^{\mathrm{c}} &= 1/[2(n+\theta)], \quad i = 1, \ldots, 2n, \end{aligned} \tag{11}$$

where scalar θ is a scale parameter, α, β, κ are method parameters, and $\theta = \alpha^2(n+\kappa) - n$.

The prediction equations of UIF are different from unscented Kalman filter (UKF),

$$\boldsymbol{Y}_{k+1|k} = (\boldsymbol{P}_{k+1|k})^{-1}, \tag{12}$$

$$\hat{\boldsymbol{y}}_{k+1|k} = \boldsymbol{Y}_{k+1|k} \sum_{i=0}^{2n} W_i^{\mathrm{m}} \boldsymbol{\chi}_{i,k+1}^{x}, \tag{13}$$

where $\boldsymbol{Y}_{k+1|k}$ and $\hat{\boldsymbol{y}}_{k+1|k}$ are the predicted information covariance and state vector, respectively. The predicted sigma point vector $\boldsymbol{\chi}_{i,k+1}^{x} = f(\boldsymbol{\chi}_{i,k}^{x}, \boldsymbol{\chi}_{i,k}^{w}, k)$; therefore, the predicted state covariance matrix can be calculated by

$$\boldsymbol{P}_{k+1|k} = \sum_{i=0}^{2n} W_i^{\mathrm{c}} (\boldsymbol{\chi}_{i,k+1}^{x} - \hat{\boldsymbol{x}}_{k+1|k})(\boldsymbol{\chi}_{i,k+1}^{x} - \hat{\boldsymbol{x}}_{k+1|k})^{\mathrm{T}}. \tag{14}$$

In the error-propagation step, the observation covariance and cross-correlation covariance are

$$\boldsymbol{P}_{k+1|k}^{\mathrm{z,z}} = E\left[(\boldsymbol{z}_{k+1} - \hat{\boldsymbol{z}}_{k+1|k})(\boldsymbol{z}_{k+1} - \hat{\boldsymbol{z}}_{k+1|k})^{\mathrm{T}}\right] \simeq \boldsymbol{H}_{k+1} \boldsymbol{P}_{k+1|k} \boldsymbol{H}_{k+1}^{\mathrm{T}}, \tag{15}$$

$$\boldsymbol{P}_{k+1|k}^{\mathrm{x,z}} = E\left[(\boldsymbol{x}_{k+1} - \hat{\boldsymbol{x}}_{k+1|k})(\boldsymbol{z}_{k+1} - \hat{\boldsymbol{z}}_{k+1|k})^{\mathrm{T}}\right] \simeq \boldsymbol{P}_{k+1} \boldsymbol{H}_{k+1}^{\mathrm{T}}, \tag{16}$$

where $\boldsymbol{z}_k = h(\boldsymbol{x}_k)$ and $\boldsymbol{H}_{k+1}$ denotes the linearized measurement matrix. Based on (15) and (16), the information state contribution $\boldsymbol{i}_{k+1}$ and its information matrix $\boldsymbol{I}_{k+1}$ are given by

$$\boldsymbol{i}_{k+1} = (\boldsymbol{P}_{k+1|k})^{-1}\boldsymbol{P}^{\mathrm{x,z}}_{k+1|k}\boldsymbol{R}^{-1}_{k+1}\left[\boldsymbol{v}_{k+1} + (\boldsymbol{P}^{\mathrm{x,z}}_{k+1|k})^{\mathrm{T}}(\boldsymbol{P}_{k+1|k})^{-\mathrm{T}}\hat{\boldsymbol{x}}_{k+1|k}\right], \tag{17}$$

$$\boldsymbol{I}_{k+1} = (\boldsymbol{P}_{k+1|k})^{-1}\boldsymbol{P}^{\mathrm{x,z}}_{k+1}\boldsymbol{R}^{-1}_{k+1}(\boldsymbol{P}^{\mathrm{x,z}}_{k+1})^{\mathrm{T}}(\boldsymbol{P}_{k+1|k})^{-1}. \tag{18}$$

We define the pseudo-measurement matrix $\boldsymbol{\Psi}_{k+1}$ satisfying $\boldsymbol{\Psi}^{\mathrm{T}}_{k+1} = (\boldsymbol{P}_{k+1|k})^{-1}\boldsymbol{P}^{\mathrm{x,z}}_{k+1|k}$. Hence, the information contribution equations are

$$\begin{cases} \boldsymbol{i}_{k+1} = \boldsymbol{\Psi}^{\mathrm{T}}_{k+1}\boldsymbol{R}^{-1}_{k+1}(\boldsymbol{v}_{k+1} + \boldsymbol{\Psi}_{k+1}\hat{\boldsymbol{x}}_{k+1|k}), \\ \boldsymbol{I}_{k+1} = \boldsymbol{\Psi}^{\mathrm{T}}_{k+1}\boldsymbol{R}^{-1}_{k+1}\boldsymbol{\Psi}_{k+1}. \end{cases} \tag{19}$$

Therefore,

$$\boldsymbol{z}_{k+1} = h(\boldsymbol{x}_{k+1}, k+1) \simeq \boldsymbol{\Psi}_{k+1}\boldsymbol{x}_{k+1} + \tilde{\boldsymbol{u}}_{k+1}, \tag{20}$$

$$\hat{\boldsymbol{x}}_{k+1|k+1} = \boldsymbol{P}_{k+1|k+1}\hat{\boldsymbol{y}}_{k+1|k+1}, \tag{21}$$

where $\tilde{\boldsymbol{u}}_{k+1} = h(\hat{\boldsymbol{x}}_{k+1|k}) - \boldsymbol{\Psi}_{k+1}\hat{\boldsymbol{x}}_{k+1|k}$.

3.2 UIF-based cooperative tracking algorithm

By considering sensor faults, we assume that the sensor of node i fails during the course of tracking. The update equations for the distributed nonlinear estimation are

$$\boldsymbol{Y}^i_k = \boldsymbol{Y}^i_{k|k-1} + \lambda^i_k\boldsymbol{I}^i_k + \sum_{j\in\boldsymbol{N}_i}\lambda^j_k\boldsymbol{I}^j_k, \tag{22}$$

$$\hat{\boldsymbol{y}}^i_k = \hat{\boldsymbol{y}}^i_{k|k-1} + \lambda^i_k\boldsymbol{i}^i_k + \sum_{j\in\boldsymbol{N}_i}\lambda^j_k\boldsymbol{i}^j_k, \tag{23}$$

where $\boldsymbol{N}_i$ represents the set of neighbor nodes of the i-th node.

The typical form of the distributed consensus method is:

$$\boldsymbol{\zeta}^i(l+1) = W^{i,i}\boldsymbol{\zeta}^i(l) + \sum_{j\in\boldsymbol{N}_i}W^{i,j}\boldsymbol{\zeta}^j(l), \tag{24}$$

where $W^{i,j}$ denotes the weight of $\boldsymbol{\zeta}^j$ to the i-th node, and satisfies $\boldsymbol{W}\boldsymbol{1} = \boldsymbol{1}$ herein based on the weighted average consensus theory [23].

In the UIF-based cooperative tracking algorithm with sensor faults, each node i must collect the measurements $\boldsymbol{z}^i_k$ from all the neighboring nodes, and exchange the information contribution matrices $\boldsymbol{I}_k$ and $\boldsymbol{i}_k$ with its neighbors $j \in \boldsymbol{N}_i$. We obtained the local estimation based on (22) and (23), and performed the integration

$$\begin{cases} \hat{\boldsymbol{y}}^i_{k,l+1} = \omega^{i,i}_k\hat{\boldsymbol{y}}^i_{k,l} + \sum_{j\in\boldsymbol{N}_i}\omega^{i,j}_k\hat{\boldsymbol{y}}^j_{k,l}, \\ \boldsymbol{Y}^i_{k,l+1} = \omega^{i,i}_k\boldsymbol{Y}^i_{k,l} + \sum_{j\in\boldsymbol{N}_i}\omega^{i,j}_k\boldsymbol{Y}^j_{k,l}, \end{cases} \tag{25}$$

in which the consensus iteration is initialized by $\hat{\boldsymbol{y}}^i_{k,0} = \hat{\boldsymbol{y}}^i_k$, $\hat{\boldsymbol{Y}}^i_{k,0} = \hat{\boldsymbol{Y}}^i_k$, $l = 0, 1, \ldots, L-1$ (L is the number of consensus step).

Therefore, the state estimation can be expressed as

$$\hat{\boldsymbol{x}}^i_k = (\boldsymbol{Y}^i_k)^{-1}\hat{\boldsymbol{y}}^i_k, \tag{26}$$

where $\hat{\boldsymbol{y}}^i_k = \hat{\boldsymbol{y}}^i_{k,L}$, $\boldsymbol{Y}^i_k = \boldsymbol{Y}^i_{k,L}$.

3.3 Stochastic boundedness analysis

As in the previous work, the stochastic boundedness of the filtering estimation error in mean square is introduced to evaluate the filtering method's performance. Because sensor faults cause changes in the estimation equations, the feasibility of the consensus algorithm must also be investigated.

First, we define a pseudo-system matrix $\boldsymbol{F}_{k-1}^i$ and an observation matrix $\boldsymbol{H}_k^i$ as follows:

$$\boldsymbol{F}_{k-1}^i = (\boldsymbol{P}_{\boldsymbol{x}_{k-1}\boldsymbol{x}_{k|k-1}}^i)^{\mathrm{T}}(\boldsymbol{P}_{k-1}^i)^{-1}, \tag{27}$$

$$\boldsymbol{H}_k^i = (\boldsymbol{P}_{\boldsymbol{x}_k\boldsymbol{z}_k}^i)^{\mathrm{T}}(\boldsymbol{P}_{k|k-1}^i)^{-1}. \tag{28}$$

We introduce the compensation instrumental diagonal matrices $\boldsymbol{\alpha}_k^i = \mathrm{diag}(\alpha_{k,1}^i, \ldots, \alpha_{k,n}^i)$ and $\boldsymbol{\beta}_k^i = \mathrm{diag}(\beta_{k,1}^i, \ldots, \beta_{k,n}^i)$ to neutralize the approximation error.

Then nonlinear system's equations are shown as

$$\begin{cases} \boldsymbol{x}_k = \boldsymbol{\alpha}_{k-1}^i \boldsymbol{F}_{k-1}^i \boldsymbol{x}_{k-1} + \boldsymbol{w}_{k-1}, \\ \boldsymbol{z}_k^i = \lambda_k^i \boldsymbol{\beta}_k^i \boldsymbol{H}_k^i \boldsymbol{x}_k + \boldsymbol{v}_k^i. \end{cases} \tag{29}$$

To demonstrate the stochastic boundedness of the estimation error, the stochastic stability lemma in [27] is introduced herein.

Lemma 1. It is assumed that ζ_k denotes the stochastic process, and there exists another process $V_k(\zeta_k)$ such that for $\forall k$,

$$\underline{p}\|\zeta_k\|^2 \leqslant V(\zeta_k) \leqslant \bar{p}\|\zeta_k\|^2, \tag{30}$$

$$E\left\{V_{k+1}(\zeta_{k+1})|\zeta_k\right\} - V_k(\zeta_k) \leqslant \mu - \varepsilon V_k(\zeta_k), \tag{31}$$

where $\underline{p},\ \bar{p},\ \mu,\ \varepsilon$ are positive real numbers and $\varepsilon \leqslant 1$.

Consequently, the stochastic process is exponentially bounded in mean square. Therefore,

$$E\left\{\|\zeta_k\|^2\right\} \leqslant \frac{\bar{p}}{\underline{p}} E\left\{\|\zeta_0\|^2\right\}(1-\varepsilon)^k + \frac{\mu}{\underline{p}} \sum_{i=1}^{k-1} (1-\varepsilon)^i. \tag{32}$$

Based on Lemma 1, three assumptions that are standard, reasonable, and typically used in the related literatures [16,17,25–27], are made for the stability analysis of the unscented information filtering method before the proof of the stochastic boundedness.

Assumption 1. There are some nonzero real numbers $\underline{\alpha},\ \bar{\alpha},\ \underline{f},\ \bar{f},\ \underline{\beta},\ \bar{\beta},\ \underline{h},\ \bar{h}$ such that the following inequalities hold for $k \geqslant 1$:

$$\underline{\alpha}^2 \boldsymbol{I} \leqslant \boldsymbol{\alpha}_k^i (\boldsymbol{\alpha}_k^i)^{\mathrm{T}} \leqslant \bar{\alpha}^2 \boldsymbol{I}, \quad \underline{f}^2 \boldsymbol{I} \leqslant \boldsymbol{F}_k^i (\boldsymbol{F}_k^i)^{\mathrm{T}} \leqslant \bar{f}^2 \boldsymbol{I},$$

$$\underline{\beta}^2 \boldsymbol{I} \leqslant \boldsymbol{\beta}_k^i (\boldsymbol{\beta}_k^i)^{\mathrm{T}} \leqslant \bar{\beta}^2 \boldsymbol{I}, \quad \underline{h}^2 \boldsymbol{I} \leqslant \boldsymbol{H}_k^i (\boldsymbol{H}_k^i)^{\mathrm{T}} \leqslant \bar{h}^2 \boldsymbol{I}.$$

Assumption 2. There are some positive real constants $\underline{q},\ \bar{q},\ \underline{r},\ \bar{r}$ such that the following inequalities are fulfilled for $k \geqslant 1$:

$$\underline{q}\boldsymbol{I} \leqslant \boldsymbol{Q}_k \leqslant \bar{q}\boldsymbol{I}, \quad \underline{r}\boldsymbol{I} \leqslant \boldsymbol{R}_k^i \leqslant \bar{r}\boldsymbol{I}.$$

Assumption 3. Suppose that there exist scalars $\underline{s}, \bar{s} > 0$ such that

$$\underline{s}\boldsymbol{I} \leqslant \boldsymbol{Y}_k^i \leqslant \bar{s}\boldsymbol{I},$$

when $i \in N$ and $k \geqslant 1$.

Based on the assumptions above, the modified predicted error covariance can be described as

$$\boldsymbol{P}_{k|k-1}^i = \boldsymbol{\alpha}_{k-1}^i \boldsymbol{F}_{k-1}^i \boldsymbol{P}_{k-1}^i (\boldsymbol{\alpha}_{k-1}^i \boldsymbol{F}_{k-1}^i)^{\mathrm{T}} + \boldsymbol{Q}_{k-1}. \tag{33}$$

Theorem 1. For the mobile sensor networks described by (2) that satisfies all the assumptions above, the estimation error of the UIF-based cooperative tracking algorithm proposed herein is exponentially bounded in mean square.

Proof. First, we consider the following definitions: the prediction error $\tilde{\boldsymbol{x}}^i_{k+1|k} = \boldsymbol{x}_{k+1} - \hat{\boldsymbol{x}}^i_{k+1|k}$, the estimation error $\tilde{\boldsymbol{x}}^i_k = \boldsymbol{x}_k - \hat{\boldsymbol{x}}^i_k$, $\tilde{\boldsymbol{x}}_{k+1|k} = \mathrm{col}(\tilde{\boldsymbol{x}}^i_{k+1|k})$ and $\tilde{\boldsymbol{x}}_k = \mathrm{col}(\tilde{\boldsymbol{x}}^i_k)$. We suppose that the Perron–Frobenius left eigenvector of $\boldsymbol{W}^L$ is given by $\boldsymbol{P} = (p^1, \ldots, p^N)^{\mathrm{T}}$, and satisfies $\sum_{j\in N} p^j \omega^{i,j}_L = p^i$.

We then discuss the following stochastic process:

$$V(\tilde{\boldsymbol{x}}_{k+1|k}) = \sum_{i\in N} p^i (\tilde{\boldsymbol{x}}^i_{k+1|k})^{\mathrm{T}} \boldsymbol{Y}^i_{k+1|k} \tilde{\boldsymbol{x}}^i_{k+1|k}. \tag{34}$$

The following bounds are fulfilled:

$$p_{\min}\underline{s}\left\|\tilde{\boldsymbol{x}}_{k+1|k}\right\|^2 \leqslant V(\tilde{\boldsymbol{x}}_{k+1|k}) \leqslant p_{\max}\bar{s}\left\|\tilde{\boldsymbol{x}}_{k+1|k}\right\|^2. \tag{35}$$

It is known that $\tilde{\boldsymbol{x}}^i_{k+1|k} = \boldsymbol{x}_{k+1} - \hat{\boldsymbol{x}}^i_{k+1|k}$. Therefore, we obtain

$$\begin{aligned}
\tilde{\boldsymbol{x}}^i_{k+1|k} &= \boldsymbol{\alpha}^i_k \boldsymbol{F}^i_k (\boldsymbol{x}_k - \hat{\boldsymbol{x}}^i_k) + \boldsymbol{w}_k \\
&= \sum_{j\in N} \omega^{i,j}_L \boldsymbol{\alpha}^i_k \boldsymbol{F}^i_k (\boldsymbol{Y}^i_k)^{-1} \boldsymbol{Y}^j_{k|k-1} \tilde{\boldsymbol{x}}^j_{k|k-1} - \sum_{j\in N} \omega^{i,j}_L \boldsymbol{\alpha}^i_k \boldsymbol{F}^i_k (\boldsymbol{Y}^i_k)^{-1} (\lambda^j_k \boldsymbol{\beta}^j_k \boldsymbol{H}^j_k)^{\mathrm{T}} (\boldsymbol{R}^j_k)^{-1} \boldsymbol{v}^j_k + \boldsymbol{w}_k \\
&= \sum_{j\in N} \boldsymbol{\Gamma}^{i,j}_k \tilde{\boldsymbol{x}}^j_{k|k-1} + \sum_{j\in N} \boldsymbol{\Theta}^{i,j}_k \boldsymbol{v}^j_k + \boldsymbol{w}_k.
\end{aligned} \tag{36}$$

In the formula above,

$$\begin{aligned}
\boldsymbol{\Gamma}^{i,j}_k &= \omega^{i,j}_L \boldsymbol{\alpha}^i_k \boldsymbol{F}^i_k (\boldsymbol{Y}^i_k)^{-1} \boldsymbol{Y}^j_{k|k-1}, \\
\boldsymbol{\Theta}^{i,j}_k &= -\omega^{i,j}_L \boldsymbol{\alpha}^i_k \boldsymbol{F}^i_k (\boldsymbol{Y}^i_k)^{-1} (\lambda^j_k \boldsymbol{\beta}^j_k \boldsymbol{H}^j_k)^{\mathrm{T}} (\boldsymbol{R}^j_k)^{-1}.
\end{aligned}$$

Therefore, we obtain

$$E\left\{V(\tilde{\boldsymbol{x}}_{k+1|k}) | \tilde{\boldsymbol{x}}_{k|k-1}\right\} = \boldsymbol{\Phi}^{\mathrm{x}}_{k+1} + \boldsymbol{\Phi}^{\mathrm{v}}_{k+1} + \boldsymbol{\Phi}^{\mathrm{w}}_{k+1}, \tag{37}$$

where

$$\boldsymbol{\Phi}^{\mathrm{x}}_{k+1} = E\left\{\sum_{i\in N} p^i \left(\sum_{j\in N} \boldsymbol{\Gamma}^{i,j}_k \tilde{\boldsymbol{x}}^j_{k|k-1}\right)^{\mathrm{T}} \boldsymbol{Y}^i_{k+1|k} \left(\sum_{j\in N} \boldsymbol{\Gamma}^{i,j}_k \tilde{\boldsymbol{x}}^j_{k|k-1}\right) \middle| \tilde{\boldsymbol{x}}_{k|k-1}\right\},$$

$$\boldsymbol{\Phi}^{\mathrm{v}}_{k+1} = E\left\{\sum_{i\in N} p^i \left(\sum_{j\in N} \boldsymbol{\Theta}^{i,j}_k \boldsymbol{v}^j_k\right)^{\mathrm{T}} \boldsymbol{Y}^i_{k+1|k} \left(\sum_{j\in N} \boldsymbol{\Theta}^{i,j}_k \boldsymbol{v}^j_k\right) \middle| \tilde{\boldsymbol{x}}_{k|k-1}\right\},$$

$$\boldsymbol{\Phi}^{\mathrm{w}}_{k+1} = E\left\{\sum_{i\in N} p^i \boldsymbol{w}^{\mathrm{T}}_k \boldsymbol{Y}^i_{k+1|k} \boldsymbol{w}_k \middle| \tilde{\boldsymbol{x}}_{k|k-1}\right\}.$$

Based on (33) and (37), we obtain ($\tau < 1$)

$$\boldsymbol{Y}^i_{k+1|k} = \left(\boldsymbol{\alpha}^i_k \boldsymbol{F}^i_k (\boldsymbol{Y}^i_k)^{-1} (\boldsymbol{\alpha}^i_k \boldsymbol{F}^i_k)^{\mathrm{T}} + \boldsymbol{Q}_k\right)^{-1} \leqslant \tau (\boldsymbol{\alpha}^i_k \boldsymbol{F}^i_k)^{-\mathrm{T}} \boldsymbol{Y}^i_k (\boldsymbol{\alpha}^i_k \boldsymbol{F}^i_k)^{-1}, \tag{38}$$

$$\boldsymbol{\Phi}^{\mathrm{x}}_{k+1} \leqslant \tau E\left\{\sum_{i\in N} p^i \left(\sum_{j\in N} \omega^{i,j}_L \boldsymbol{Y}^j_{k|k-1} \tilde{\boldsymbol{x}}^j_{k|k-1}\right)^{\mathrm{T}} \boldsymbol{Y}^i_k \sum_{j\in N} \omega^{i,j}_L \boldsymbol{Y}^j_{k|k-1} \tilde{\boldsymbol{x}}^j_{k|k-1}\right\}. \tag{39}$$

Because $\boldsymbol{Y}^i_k \geqslant \sum_{j\in\{\boldsymbol{N}_i, i\}} \omega^{i,j}_L \boldsymbol{Y}^j_{k|k-1}$, hence $\boldsymbol{\Phi}^{\mathrm{x}}_{k+1}$ satisfies

$$\boldsymbol{\Phi}^{\mathrm{x}}_{k+1} \leqslant \tau E\left\{\sum_{i\in N} p^i \sum_{j\in N} \omega^{i,j}_L (\tilde{\boldsymbol{x}}^j_{k|k-1})^{\mathrm{T}} \boldsymbol{Y}^j_{k|k-1} \tilde{\boldsymbol{x}}^j_{k|k-1}\right\} \leqslant \tau E\left\{\sum_{j\in N} p^j (\tilde{\boldsymbol{x}}^j_{k|k-1})^{\mathrm{T}} \boldsymbol{Y}^j_{k|k-1} \tilde{\boldsymbol{x}}^j_{k|k-1}\right\}$$

$$= (1-\varepsilon)E[V(\tilde{\boldsymbol{x}}_{k+1|k})], \tag{40}$$

in which $\varepsilon = 1-\tau$.

Furthermore,

$$\begin{aligned}&\boldsymbol{\Phi}^{\mathrm{v}}_{k+1} + \boldsymbol{\Phi}^{\mathrm{w}}_{k+1}\\ &= E\left\{\sum_{i\in N} p^i \left(\sum_{j\in N} \boldsymbol{\Theta}^{i,j}_k \boldsymbol{v}^j_k\right)^{\mathrm{T}} \boldsymbol{Y}^i_{k+1|k} \left(\sum_{j\in N} \boldsymbol{\Theta}^{i,j}_k \boldsymbol{v}^j_k\right) + \sum_{i\in N} p^i \boldsymbol{w}^{\mathrm{T}}_k \boldsymbol{Y}^i_{k+1|k} \boldsymbol{w}_k \,\middle|\, \tilde{\boldsymbol{x}}_{k|k-1}\right\}.\end{aligned} \tag{41}$$

It is noteworthy that Eq. (33) can be rewritten as

$$\boldsymbol{Y}^i_{k|k-1} = \left(\boldsymbol{\alpha}^i_{k-1}\boldsymbol{F}^i_{k-1}(\boldsymbol{Y}^i_{k-1})^{-1}(\boldsymbol{\alpha}^i_{k-1}\boldsymbol{F}^i_{k-1})^{\mathrm{T}} + \boldsymbol{Q}_{k-1}\right)^{-1}. \tag{42}$$

Suppose that $\boldsymbol{Y}^i_{k+1|k} \leqslant s\boldsymbol{I}$. Then

$$\boldsymbol{\Phi}^{\mathrm{v}}_{k+1} + \boldsymbol{\Phi}^{\mathrm{w}}_{k+1} \leqslant s\left\{\underline{s}^{-1}\bar{\alpha}^2\bar{f}^2\bar{\beta}^2\bar{h}^2\left[\sum_{i,j\in N} p^i(\omega^{i,j}_L)^2\right] m + \bar{q}\left(\sum_{i\in N} p^i\right) n\right\} \triangleq \mu, \tag{43}$$

in which m and n refer to the dimensions of $\boldsymbol{z}^i_k$ and $\boldsymbol{x}_k$, respectively.

It follows from (40) and (43) that

$$E\left\{V(\tilde{\boldsymbol{x}}_{k+1|k})|\tilde{\boldsymbol{x}}_{k|k-1}\right\} - V(\tilde{\boldsymbol{x}}_{k|k-1}) \leqslant \mu - \varepsilon V(\tilde{\boldsymbol{x}}_{k|k-1}). \tag{44}$$

Based on Lemma 1 mentioned previously, we conclude that the stochastic process $\tilde{\boldsymbol{x}}_{k+1|k}$ and $\tilde{\boldsymbol{x}}^i_{k+1|k}$ for each node all are exponentially bounded in mean square.

According to (36), one obtains

$$E\left\{\|\tilde{\boldsymbol{x}}^i_k\|^2\right\} \leqslant \underline{\alpha}^{-2}\underline{f}^{-2}\left(E\left\{\|\tilde{\boldsymbol{x}}^i_{k+1|k}\|^2\right\} - E\left\{\|\boldsymbol{w}^i_k\|^2\right\}\right). \tag{45}$$

In conclusion, for the nonlinear multi-agent systems described in (2) that satisfy all the assumptions above, the estimation error $\tilde{\boldsymbol{x}}^i_{k+1|k}$ of the UIF-based cooperative tracking algorithm proposed herein is exponentially bounded in mean square. This proof is completed.

Remark 1. The system's state matrix and observation matrix are approximated to help solve the problems caused by nonlinearity, and reduce the computational complexity, which refers to the statistical linear regression method in [17, 23]. Unlike the filtering method in [23], the data fusion is processed before the consensus iterations in the UIF-based cooperative tracking algorithm, to obtain more precise estimates.

4 Illustrative example

Two mathematical simulations are provided herein to discuss the problem in the cooperative tracking method. The performance of the UIF-based cooperative tracking algorithm proposed herein is demonstrated in Example 1. Example 2 illustrates the interactive multiple model (IMM)-UIF cooperative tracking method in three dimensions to discuss the further research work in this field.

Example 1. Suppose that a nonlinear multi-agent system is composed of four independent nodes that are working collaboratively to track a single maneuvering target. The motion of the target can be described by the turn manoeuver in the two-dimensional plane. The mobile sensor networks are assumed to include three static nodes and one moving node. Each node provides its measurements regarding

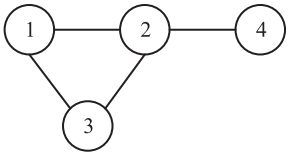

Figure 1 Communication topology of 4 nodes.

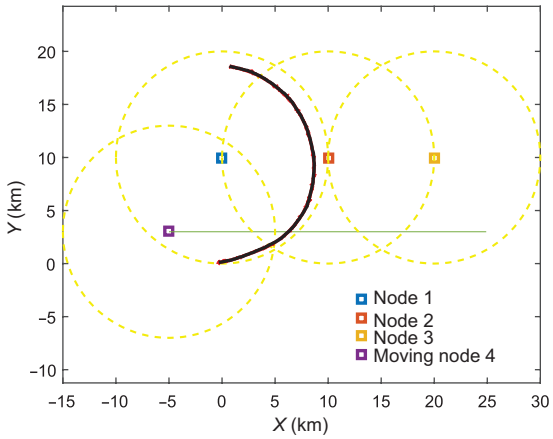

Figure 2 (Color online) Tracking trajectory of proposed method considering sensor faults.

the target (distance r_k^i and heading θ_k^i), and shares the information within the group based on the communication topology illustrated in Figure 1. The observation equation for node i is given by

$$\boldsymbol{z}_k^i = \lambda_k^i \begin{bmatrix} r_k^i \\ \theta_k^i \end{bmatrix} = \lambda_k^i \begin{bmatrix} \sqrt{(\xi_k - x_k^i)^2 + (\eta_k - y_k^i)^2} \\ \arctan \dfrac{\eta_k - y_k^i}{\xi_k - x_k^i} \end{bmatrix} + \boldsymbol{v}_k^i,$$

where (ξ_k, η_k) represents the target's position components in the X and Y directions at time k, respectively; (x_k^i, y_k^i) refers to the position of node i; $\boldsymbol{v}_k^i$ represents the measurement noise of node i with covariance $\boldsymbol{R}_k^i$.

The initial target's state variable is chosen as $\boldsymbol{x}_0 = [\xi_0, \dot{\xi}_0, \eta_0, \dot{\eta}_0]^{\mathrm{T}} = [-0.4 \text{ km}, 0.08 \text{ km/s}, 0.1 \text{ km}, 0.01 \text{ km/s}]^{\mathrm{T}}$, while $(x_0^1, y_0^1) = (0, 10 \text{ km})$, $(x_0^2, y_0^2) = (10 \text{ km}, 10 \text{ km})$, $(x_0^3, y_0^3) = (20 \text{ km}, 10 \text{ km})$. The initial position of node 4 is $(-5 \text{ km}, 3 \text{ km})$, and node 4 moves along the X axis with a constant velocity 0.1 km/s. The sampling interval T is 1 s, and the target has moved 300 s in total.

The tracking performance is reflected by the root mean square error (RMSE)

$$\mathrm{RMSE}_k = \left\{ \frac{1}{S} \sum_{l=1}^{S} \left[(\xi_{k,l} - \hat{\xi}_{k,l}^i)^2 + (\eta_{k,l} - \hat{\eta}_{k,l}^i)^2 \right] \right\}^{1/2},$$

where $(\xi_{k,l}, \eta_{k,l})$ and $(\hat{\xi}_{k,l}^i, \hat{\eta}_{k,l}^i)$ denote the true values of target's state and the estimates provided by node i, respectively; S is the number of Monte Carlo runs.

As illustrated in Figure 2, the green line is the trajectory of the moving sensor, the four dotted yellow circles represent the communication range of each node, the red line refers to the target's trajectory, and the black line represents the tracking trajectory obtained by the UIF-based cooperative tracking method considering sensor faults ($\delta = 0.5$). Furthermore, Figures 3 and 4 are plotted in the same scenario to analyze the tracking precision of the algorithm by the RMSE.

The tracking performances of a similar node whose sensor is operating in the normal or failure condition are compared in Figure 3. The result intuitively shows that sensor faults will cause a remarkable negative influence on the target state estimation. Figure 4 illustrates the estimation results regarding the UIF method of each node and the UIF-based cooperative tracking method. We found that the cooperative tracking method fusing all the neighboring nodes' measurements exhibits better tracking performance compared with the filtering algorithm of the single node. Meanwhile, the results indicate that the algorithm can improve the estimation precision for multi-agent systems with sensor failures when tracing the maneuvering target.

As shown in Figure 5, the estimation errors of three filtering methods based on the weighted average consensus theory are compared in the sensor faults case with $\delta = 0.5$, and the UIF-based cooperative

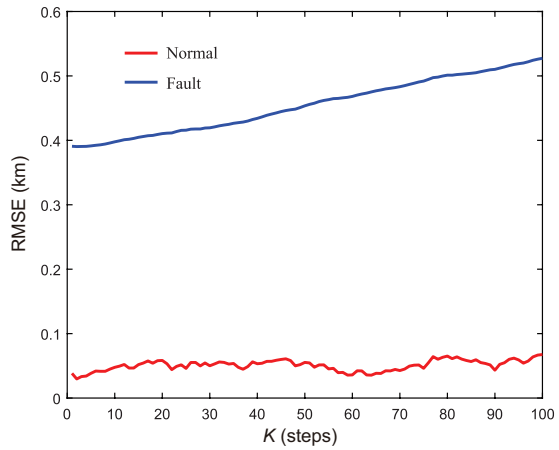

Figure 3 (Color online) Comparison between normal and fault condition.

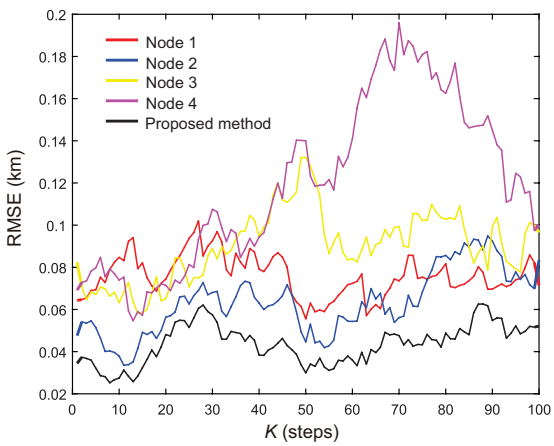

Figure 4 (Color online) RMSE of single node and the proposed method.

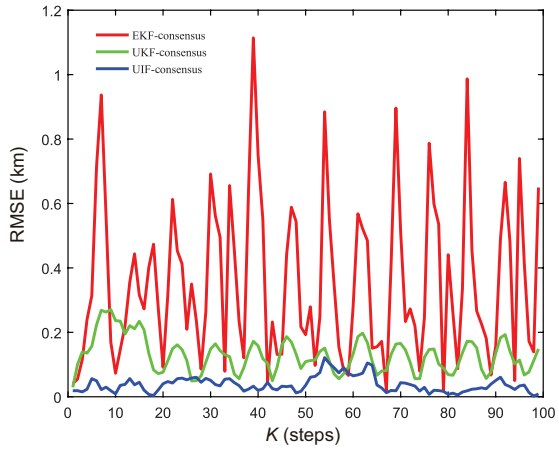

Figure 5 (Color online) Comparison of three filtering methods ($\delta = 0.5$).

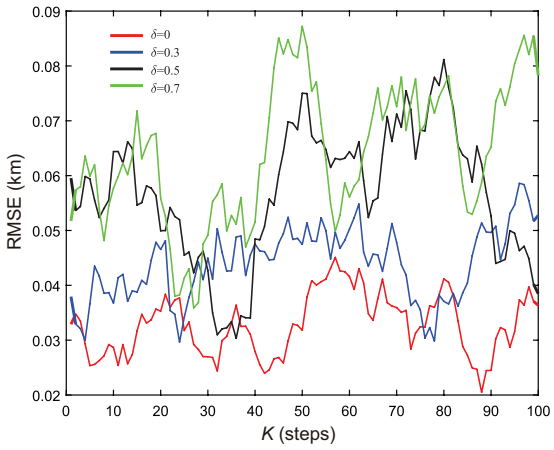

Figure 6 (Color online) Comparison of different fault conditions.

tracking algorithm is proven to demonstrate better performance in nonlinear target tracking than the other ones. It is noteworthy that the distributed consensus extend Kalman filter (EKF) and distributed UKF are typically used by previous researchers (reported in [23, 24], respectively).

As the tracking accuracy of the proposed filter is related to the value of observational probability δ, which represents the fault situation, several simulation experiments are performed when δ is chosen as $[0, 0.3, 0.5, 0.7]$. Figure 6 indicates that with the increase in δ, the tracking performance becomes worse.

Example 2. Suppose that a nonlinear multi-agent system is composed of 10 independent nodes that are operating collaboratively to track a single maneuvering target. The motion of the target is described by a simulated ballistic trajectory as a S curve in a three-dimensional case. The mobile sensor networks are assumed to include five static nodes and five moving nodes, with the communication topology illustrated in Figure 7. The communication range of each node is set as 850 km. The sampling interval T is 1 s, and the target has moved 600 s in total. Owing to space limitations herein, the interactive multiple model is not elaborated. The model set consists of the constant velocity model, constant acceleration model, and current statistical model.

As shown in Figure 8, the red curve refers to the real target trajectory. The green line represents the position estimation results of a single node adopting the IMM-UIF method, the sensor of which is operating in the failure ($\delta = 0.5$) condition. Obviously, the tracking performance is poor owing to the

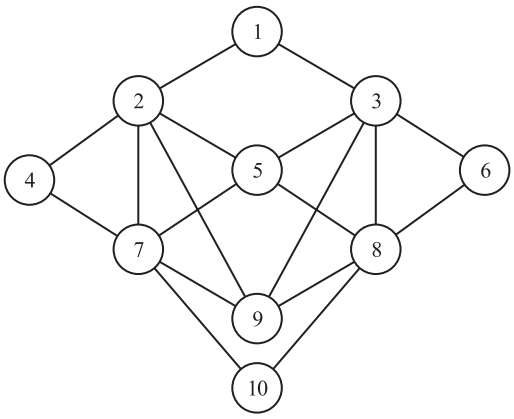

Figure 7 Communication topology of 10 nodes.

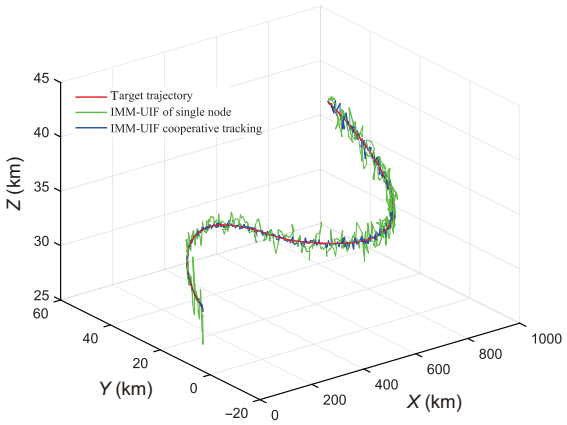

Figure 8 (Color online) Tracking performance of IMM-UIF.

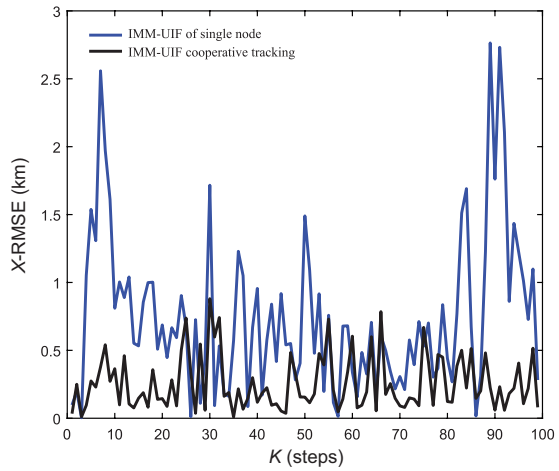

Figure 9 (Color online) RMSE of target's position estimation (X).

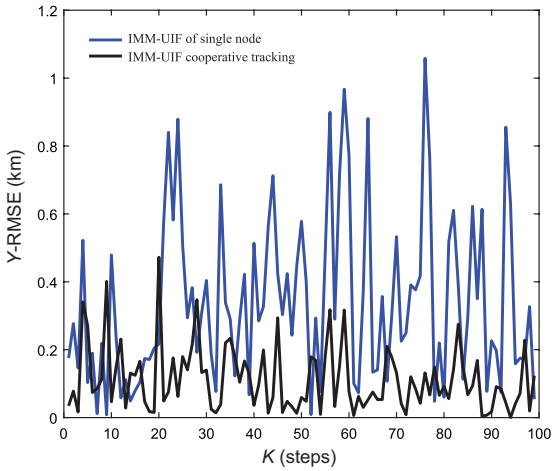

Figure 10 (Color online) RMSE of target's position estimation (Y).

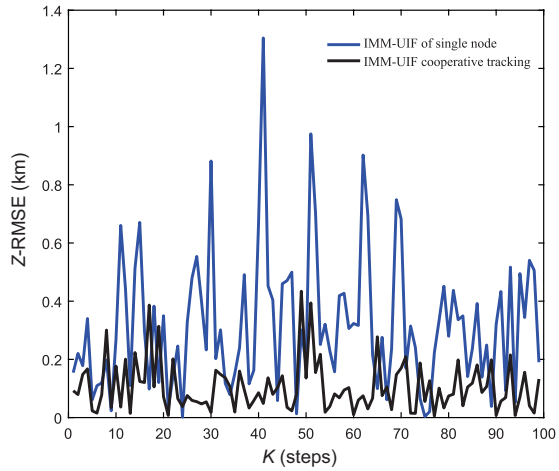

Figure 11 (Color online) RMSE of target's position estimation (Z).

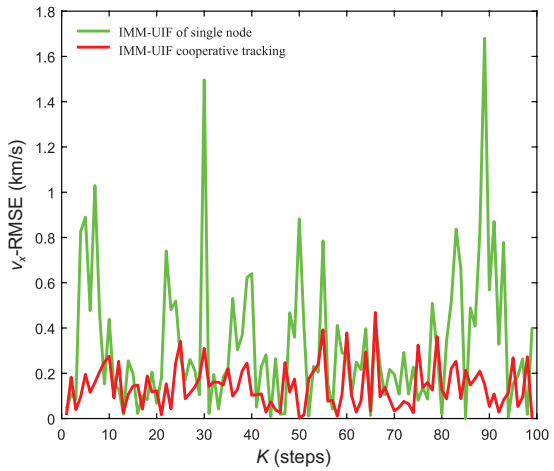

Figure 12 (Color online) RMSE of target's velocity estimation (v_x).

sensor faults. In a same scenario ($\delta = 0.5$), when the information are exchanged between the neighboring nodes, 10 nodes operate collaboratively for target tracing, and provide a better tracking curve (the blue

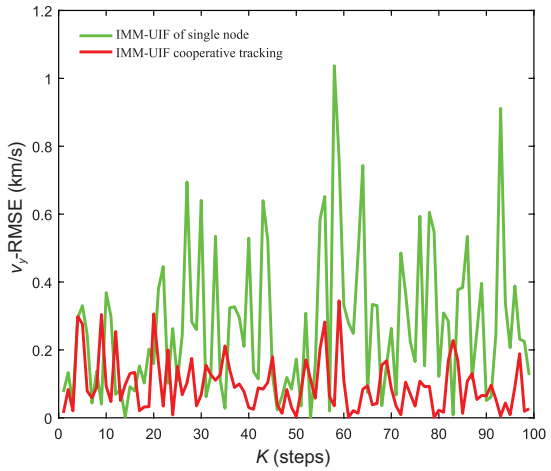

Figure 13 (Color online) RMSE of target's velocity estimation (v_y).

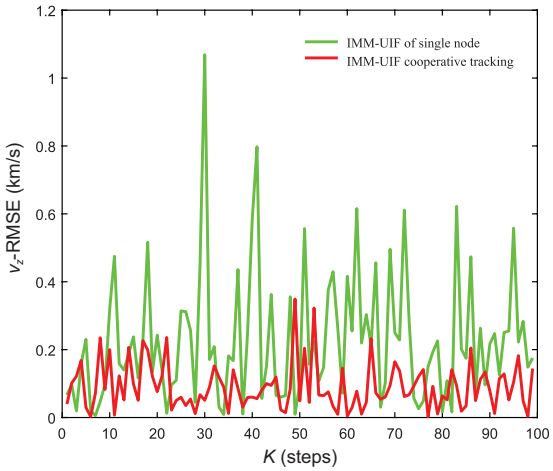

Figure 14 (Color online) RMSE of target's velocity estimation (v_z).

one) that almost coincided with that of the target trajectory. For the multi-agent systems with sensor faults, Figures 9–14 depicts the comparison of several RMSE results between the IMM-UIF method and the IMM-UIF cooperative tracking method based on the weighted average consensus theory. For a single node, the maximum of the estimation error of the position is close to 2.8 km, and the estimation error of the velocity is up to 1.7 km/s. In contrast, for the IMM-UIF cooperative tracking method, the maximum of the estimation error of the position is only 0.8 km, and the estimation error of the velocity is less than 0.4 km/s. We conclude that the method elaborated herein can improve the estimation accuracy compared with the filtering algorithm of a single node for the tracking problem with sensor faults, when the target model is described by the IMM. The algorithm's stability is still required to be proven theoretically.

5 Conclusion

A novel cooperative tracking algorithm for nonlinear estimation and multiple sensor fusion was proposed herein. The proposed information fusion method for multi-agent systems was derived by combining the advantages of the weighted average consensus theory and UIF, to solve the problem caused by sensor faults. Moreover, the stochastic boundedness of the estimation error for the discussed nonlinear system was analyzed to assess the method performance and feasibility. Future research directions include extending the proposed method to mobile sensor networks with both sensor failures and switching topologies, and directed networks. For the practical implementation of the tracking method, it is necessary to consider the problem of time delay in the filter design.

Acknowledgements This work was supported by National Natural Science Foundation of China (Grant Nos. 61873011, 61803014, 61503009, 61333011), Beijing Natural Science Foundation (Grant No. 4182035), Young Elite Scientists Sponsorship Program by CAST (Grant No. 2017QNRC001), Aeronautical Science Foundation of China (Grant Nos. 2016ZA51005, 20170151001), Special Research Project of Chinese Civil Aircraft, State Key Laboratory of Intelligent Control and Decision of Complex Systems, and Fundamental Research Funds for the Central Universities (Grant No. YWF-18-BJ-Y-73).

References

1 Sobhani B, Paolini E, Giorgetti A, et al. Target tracking for UWB multistatic radar sensor networks. IEEE J Sel Top Signal Process, 2014, 8: 125–136
2 Wu K, Cai Z, Zhao J, et al. Target tracking based on a nonsingular fast terminal sliding mode guidance law by fixed-wing UAV. Appl Sci, 2017, 7: 333
3 Chen H Y, Zhang S L, Liu M Q, et al. An artificial measurements-based adaptive filter for energy-efficient target tracking via underwater wireless sensor networks. Sensors, 2017, 17: 1–19
4 Wang Y H, Lin P, Hong Y G. Distributed regression estimation with incomplete data in multi-agent networks. Sci China Inf Sci, 2018, 61: 092202

5 Dong X, Yu B, Shi Z, et al. Time-varying formation control for unmanned aerial vehicles: theories and applications. IEEE Trans Control Syst Technol, 2015, 23: 340–348
6 Dong X W, Zhou Y, Ren Z, et al. Time-varying formation tracking for second-order multi-agent systems subjected to switching topologies with application to quadrotor formation flying. IEEE Trans Ind Electron, 2017, 64: 5014–5024
7 Dong X W, Zhou Y, Ren Z, et al. Time-varying formation control for unmanned aerial vehicles with switching interaction topologies. Control Eng Practic, 2016, 46: 26–36
8 Fang H, Shang C S, Chen J. An optimization-based shared control framework with applications in multi-robot systems. Sci China Inf Sci, 2018, 61: 014201
9 Li Z K, Ren W, Liu X D, et al. Distributed containment control of multi-agent systems with general linear dynamics in the presence of multiple leaders. Int J Robust Nonlinear Control, 2013, 23: 534–547
10 Blackman S S. Abstracts of previous tutorials in this series: multiple hypothesis tracking for multiple target tracking. IEEE Aerosp Electron Syst Mag, 2016, 31: 90–96
11 Milan A, Schindler K, Roth S. Multi-target tracking by discrete-continuous energy minimization. IEEE Trans Pattern Anal Mach Intell, 2016, 38: 2054–2068
12 Yu W W, Li C J, Yu X H, et al. Economic power dispatch in smart grids: a framework for distributed optimization and consensus dynamics. Sci China Inf Sci, 2018, 61: 012204
13 Peng Z H, Wang D, Wang H, et al. Distributed cooperative tracking of uncertain nonlinear multi-agent systems with fast learning. Neurocomputing, 2014, 129: 494–503
14 Qin J H, Ma Q C, Gao H J, et al. Fault-tolerant cooperative tracking control via integral sliding mode control technique. IEEE/ASME Trans Mechatron, 2018, 23: 342–351
15 Li J Z. Distributed cooperative tracking of multi-agent systems with actuator faults. Trans Inst Meas Control, 2015, 37: 1041–1048
16 Li W L, Jia Y M, Du J P. Distributed Kalman consensus filter with intermittent observations. J Franklin Inst, 2015, 352: 3764–3781
17 Tan Q K, Dong X W, Liu F, et al. Weighted average consensus-based cubature information filtering for mobile sensor networks with intermittent observations. In: Proceedings of Chinese Control Conference, Dalian, 2017. 8946–8951
18 Ding J L, Xiao J, Zhang Y. Distributed algorithm-based CKF and its applications to target tracking. Control Decis, 2015, 30: 296–302
19 Chen B, Ho D W C, Zhang W A, et al. Networked fusion estimation with bounded noises. IEEE Trans Autom Control, 2017, 62: 5415–5421
20 Battistelli G, Chisci L, Mugnai G, et al. Consensus-based linear and nonlinear filtering. IEEE Trans Autom Control, 2015, 60: 1410–1415
21 Zhang H S, Song X X, Shi L. Convergence and mean square stability of suboptimal estimator for systems with measurement packet dropping. IEEE Trans Autom Control, 2012, 57: 1248–1253
22 Du Y K, Ju H Y, Yong H K, et al. Distributed information fusion filter with intermittent observations. In: Proceedings of the Conference on Information Fusion, Edinburgh, 2010
23 Li W Y, Wei G L, Han F, et al. Weighted average consensus-based unscented kalman filtering. IEEE Trans Cybern, 2016, 46: 558–567
24 Battistelli G, Chisci L. Stability of consensus extended Kalman filter for distributed state estimation. Automatica, 2016, 68: 169–178
25 Li L, Xia Y Q. Stochastic stability of the unscented Kalman filter with intermittent observations. Automatica, 2012, 48: 978–981
26 Chen J, Sun J, Wang G. Stochastic stability of extended filtering for non-linear systems with measurement packet losses. IET Control Theory Appl, 2013, 7: 2048–2055
27 Reif K, Gunther S, Yaz E, et al. Stochastic stability of the discrete-time extended Kalman filter. IEEE Trans Autom Control, 1999, 44: 714–728